



# CO<sub>2</sub> hydrogenation for C<sub>2+</sub> hydrocarbon synthesis over composite catalyst using surface modified HB zeolite

Masahiro Fujiwara<sup>a,\*</sup>, Takahiro Satake<sup>a,b</sup>, Kumi Shiokawa<sup>a</sup>, Hiroaki Sakurai<sup>a</sup>

<sup>a</sup> National Institute of Advanced Industrial Science and Technology (Kansai center), 1-8-31 Midorigaoka, Ikeda, Osaka 563-8577, Japan

<sup>b</sup> Osaka Institute of Technology, 5-16-1 Omiya, Asahi-ku, Osaka 535-8585, Japan

## ARTICLE INFO

### Article history:

Received 17 February 2015

Received in revised form 6 April 2015

Accepted 2 May 2015

Available online 6 May 2015

### Keywords:

CO<sub>2</sub> hydrogenation

C<sub>2+</sub> hydrocarbons

Composite catalyst

Zeolite

Surface modification

## ABSTRACT

Synthesis of C<sub>2+</sub> hydrocarbons such as LPG (liquefied petroleum gas) from CO<sub>2</sub> is expected to reduce CO<sub>2</sub> emission by the consumption of fossil fuels. In this study, CO<sub>2</sub> hydrogenation over composite catalysts comprised of Cu–Zn–Al oxide catalyst and HB zeolite was examined for the synthesis of C<sub>2+</sub> hydrocarbons by the combination of methanol synthesis over Cu–Zn–Al oxide and concurrent conversion of methanol over HB zeolite. When a non-modified zeolite was used for the composite catalyst, the yield of C<sub>2+</sub> hydrocarbons was poor (<0.5C-mol%), which was lower than that of oxygenated compounds (methanol and dimethyl ether). The strong acid sites of zeolite for the transformation of dimethyl ether to C<sub>2+</sub> hydrocarbons were seriously deactivated. The employment of zeolites modified with 1,4-bis(hydroxydimethylsilyl) benzene remarkably improved the catalytic activity of the corresponding composite catalysts to produce C<sub>2+</sub> hydrocarbons in yields of more than 7C-mol%. The best yield of C<sub>2+</sub> hydrocarbons became approximately 12.6C-mol% under a pressure of 0.98 MPa. The disilane modification produced hydrophobic zeolites showing water contact angles more than 130°. The disilane compound was converted to some condensed aromatics during CO<sub>2</sub> hydrogenation at 300 °C, and the hydrophobicity was maintained even after the reaction. The enhanced catalytic activity is caused by suppressing the deactivation of the strong acid sites of HB zeolite with the hydrophobic surface. This improved composite catalyst will promote the production of C<sub>2+</sub> hydrocarbons from CO<sub>2</sub> even under low pressure conditions.

© 2015 Elsevier B.V. All rights reserved.

## 1. Introduction

CO<sub>2</sub> hydrogenation is now believed to be an effective measure for the reduction of CO<sub>2</sub> emission and the production of carbon compounds free from fossil fuels [1–5]. In a variety of methods for CO<sub>2</sub> hydrogenation, a composite catalyst comprised of methanol synthesis catalyst and zeolite is regarded as a promising catalytic system for the selective production of C<sub>2+</sub> hydrocarbons (hydrocarbons of carbon number more than 2) such as LPG, naphtha and gasoline [6–19], which are prevalent hydrocarbons in modern society. In these composite catalysts, a methanol synthesis catalyst and a zeolite catalyst are physically mixed to aim that methanol synthesis from CO<sub>2</sub> and methanol conversion to C<sub>2+</sub> hydrocarbons progress simultaneously in a single catalytic bed (Fig. 1). In general, methanol formation by CO<sub>2</sub> hydrogenation strongly depended on reaction pressure. The equilibrium conversion of CO<sub>2</sub> to methanol is calculated to be 0.36% at 300 °C under a pressure of 1 MPa, while the conversion increases to 1.45 (2 MPa) and 8.32% (5 MPa) with the

pressure [20]. In the composite catalyst, immediate conversion of methanol to C<sub>2+</sub> hydrocarbons shifts the equilibrium to remove the thermodynamic limitation [21]. Therefore, in principle, the production of C<sub>2+</sub> hydrocarbons over the equilibrium conversion of CO<sub>2</sub> to methanol is possible even under a pressure of 1 MPa. However, as reported in our recent paper [22], the yield of C<sub>2+</sub> hydrocarbons was only slight (less than 1C-mol%) over composite catalysts comprised of Cu–Zn–Al oxide and HB zeolite under a pressure of 0.98 MPa using a single reactor.

In our previous paper [22], CO<sub>2</sub> hydrogenation was examined using a two stage reactor, where a Cu–Zn–Al oxide and a composite catalyst are packed in the first and second reactor, respectively. The combination of the partial transformation of CO<sub>2</sub> into CO at the first reactor and the following removal of water formed in the first reactor clearly enhanced the yield of C<sub>2+</sub> hydrocarbons. However, the yield dramatically decreased to less than one-tenth without the water removal. From these results, we propose a reaction scheme of CO<sub>2</sub> hydrogenation over the composite catalyst as illustrated in Fig. 2. This scheme indicates that both the suppression of methanol decomposition to CO and the prominent methanol conversion into C<sub>2+</sub> hydrocarbons are essential for high yield production of C<sub>2+</sub> hydrocarbons. Slow methanol conversion

\* Corresponding author. Tel.: +81 72 751 9525; fax: +81 72 751 9628.  
E-mail address: [m-fujiwara@aist.go.jp](mailto:m-fujiwara@aist.go.jp) (M. Fujiwara).

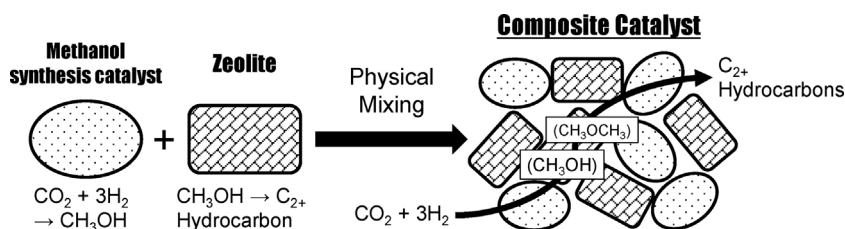


Fig. 1. Reaction scheme of  $\text{C}_2^+$  hydrocarbon synthesis over the composite catalyst composed of methanol synthesis catalyst and zeolite by  $\text{CO}_2$  hydrogenation.

over zeolite results in poor yield of  $\text{C}_2^+$  hydrocarbons, because the decomposition of methanol to CO predominantly occurs. Since the acidity of zeolite is damaged by steam during catalytic reactions [23,24], the deactivation of acid sites on the zeolite is assumed to progress by a large amount of water produced during  $\text{CO}_2$  hydrogenation. Consequently, the yield of  $\text{C}_2^+$  hydrocarbons becomes poor in usual composite catalysts. Reported high yield productions of  $\text{C}_2^+$  hydrocarbons from syngas ( $\text{CO} + \text{H}_2$ ) support the deactivation effect of water, because water formed during the reaction is efficiently eliminated by water–gas–shift reaction with CO as feed gas [6,12]. However, in the case of  $\text{CO}_2$  hydrogenation, water produced during the reaction is not removable. Therefore, new improvements are required for the composite catalyst that produces  $\text{C}_2^+$  hydrocarbons in high yield from  $\text{CO}_2$ .

Recently, hydrophobic modification of zeolites is actively studied to improve their catalytic performance and stability in water [25–27]. For example, the surface modification of HY zeolite with an octadecylsilane compound enhances the catalytic activity for biofuel upgrading reactions in aqueous solutions [26]. An improved catalytic performance of USY zeolite is also achieved by an organic modification in the alkylation of *m*-cresol [27]. Then, the hydrophobic modification of zeolite is expected to improve even the catalytic activity of the composite catalyst for  $\text{CO}_2$  hydrogenation. We have studied the grafting of organo–disilane compounds like 1,4-bis(hydroxydimethylsilyl) benzene to zeolites, which produce strong bonds with the surface by the two silanols [28–31]. When a sufficient amount of the disilane compound is grafted to mordenite and ZSM-5, it covers the whole exterior surface of the zeolites to seal their outlets of the micropores (Fig. 3). It is thought that this covering treatment with the disilane compound transforms zeolite from hydrophilic to hydrophobic, improving the catalytic activity of the corresponding composite catalyst. In this paper, we report  $\text{CO}_2$  hydrogenation under a pressure of 0.98 MPa over improved composite catalysts comprised of Cu–Zn–Al oxide and HB zeolite, whose surface was modified with 1,4-bis(hydroxydimethylsilyl) benzene.

## 2. Experimental

### 2.1. Catalyst preparations

Cu–Zn based oxide catalysts used in this study were prepared by the same procedures as our previous paper [22]. In the preparation of Cu–Zn–Al oxide (with atomic ratio 6:3:1), a mixed

1 M solution of Cu, Zn and Al nitrates (6:3:1 in molar ratio) was added at once into a 1 M solution of  $\text{Na}_2\text{CO}_3$  at  $80^\circ\text{C}$ . The amount of  $\text{Na}_2\text{CO}_3$  was 1.2 equivalents to the total stoichiometric quantities of the nitrates. The precipitate was aged for 2 h at the same temperature, then filtered and washed 5 times with a sufficient quantity of fresh deionized water. The gel thus obtained was dried at  $120^\circ\text{C}$  for 12 h and finally calcined at  $350^\circ\text{C}$  for 3 h in air.

A zeolite catalyst used here was HSZ-931HOA ( $\text{SiO}_2/\text{Al}_2\text{O}_3 = 28.5$ ) obtained from Tosoh Corporation as HB zeolite (zeolite Beta). The surface modification of the zeolite was carried out by the similar procedures to our previous papers basically [28–31]. As a typical example (for zeolite 5 in Table 1), 2 g of HB zeolite calcined at  $500^\circ\text{C}$  for 6 h was immersed in a 15 mL of methanol solution dissolving 0.2 g of 1,4-bis(hydroxydimethylsilyl) benzene purchased from Shin-Etsu Silicones, and was well mixed at room temperature for 30 min. After removing volatiles under reduced pressure using a rotary evaporator, the zeolite powder was put in a Teflon-lined autoclave. After sealing up, the autoclave was heated at  $150^\circ\text{C}$  for 24 h. The recovered solid was washed with methanol three times (150 mL each) for eliminating the disilane compound removable, and was finally dried naturally at room temperature for more than 2 days. For the preparation of zeolites 2–4, 0.02, 0.06 or 0.1 g of the disilane compound was used for the modification, respectively. In the case of zeolite 6, HB zeolite was immersed in only methanol (not containing the disilane compound). The following mixing, heating, washing and drying treatments were similar to those of zeolite 5.

Composite catalysts were prepared by grinding a powder mixture of a Cu–Zn based oxide and a zeolite in an agate mortar. Before the mixing, all zeolites were dried at  $150^\circ\text{C}$  for 3 h for removing adsorbed matters. HB zeolite calcined at  $500^\circ\text{C}$  for 6 h was used as non-modified zeolite (zeolite 1). Although we thoroughly kneaded the powder mixtures in our previous study (grinding 1000 times) [22], the mixtures were mildly grinded 100 times in this study, because the strong interaction between Cu–Zn based oxide and zeolite is claimed to damage the composite catalyst [32–35]. The weight ratio of a Cu–Zn based oxide and a zeolite was fixed to 1:9, which was ascertained to be the best in our previous study [22].

### 2.2. Catalytic tests

$\text{CO}_2$  hydrogenation was carried out by using a pressurized fixed bed flow reactor. All catalysts as smooth powders were not pelletized and directly used for catalytic reaction. In a typical catalytic test, 1 g of a composite catalyst (0.1 g of a Cu–Zn based oxide and 0.9 g of a zeolite) was loaded in a stainless-steel reactor of 10 mm inner diameter, and was reduced by pure hydrogen flow of 40 mL/min at  $250^\circ\text{C}$  approximately for 14 h under atmospheric pressure for ensuring the complete reduction of Cu oxide. After this pre-reduction, the temperature of the catalyst bed was raised to  $300^\circ\text{C}$ , and then the mixed gas of  $\text{CO}_2$  and  $\text{H}_2$  with a composition ratio of 1:3 was introduced to the reactor until the pressure was raised to 10 kgf/cm<sup>2</sup> (0.98 MPa). All parts of tubing from the outlet of the reactor to the inlet of online-gas chromatographs were heated at from 100 to  $150^\circ\text{C}$  to prevent the condensation

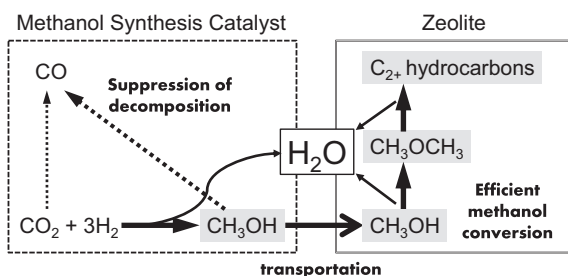


Fig. 2. Reaction steps of  $\text{CO}_2$  hydrogenation over composite catalyst (Favorable pass is shown in bold lines.).

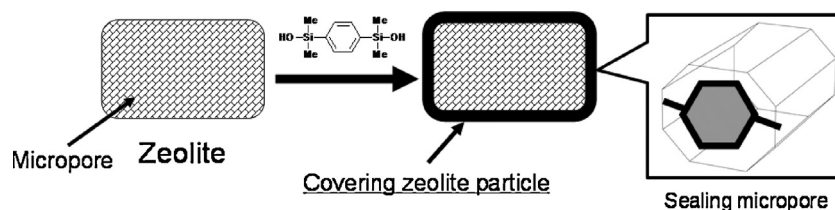


Fig. 3. Surface modification of zeolite with 1,4-bis(hydroxydimethylsilyl) benzene.

of any carbon products. All effluent compounds containing carbon were analyzed by on-line TCD and FID gas chromatographs equipped with an active carbon column for CO and CO<sub>2</sub> and with a plot column GS-Q (Shimadzu GLC) for all hydrocarbons, methanol and dimethyl ether, respectively. Calculations for evaluating the catalytic performances were based on C-mol%, which means the amount of the products based on carbon mole: [(carbon number of the product) × (yield or selectivity of the product)]. Since methane produced by the decomposition of the grafted disilane compound was detected considerably in the initial stage of the reaction as described later (in Section 3.3.), the catalytic performances at 2 h of time-on-stream are mainly used for discussion. The catalytic reactions were continued at least for 7 h under the same conditions. Both the pressure rising and reduction steps proceeded smoothly, and it is unlikely that a pressure drop through the catalyst bed occurred. All recovered composite catalysts were still smooth powders even after use in the reaction for at least 7 h. In supplementary data (Fig. S1), SEM images of a calcined HB zeolite (zeolite **1**) and a composite catalyst with zeolite **4** used for the catalytic reaction are shown. From the image of the used composite catalyst, the particles of about 5 μm in size are not agglomerated, which appear to be the same as the calcined HB zeolite.

### 2.3. Characterization

Powder X-ray diffraction analysis was performed using a Rigaku Ultima IV X-ray diffractometer with Cu-Kα radiation ( $\lambda = 0.15406$  nm). Scanning electron microscopy (SEM) images were obtained using a JEOL JSM-6390 apparatus. Infrared spectra of samples were recorded using a PerkinElmer Spectrum One spectrometer by KBr method. UV-vis spectra of solutions were analyzed by a JASCO V-530 spectrometer using standard quartz cells. Diffuse reflectance UV-vis spectra were obtained with a JASCO V-550 spectrometer equipping with an integrating sphere. Kubelka–Munk functions were plotted versus the wavelength. Nitrogen adsorption–desorption isotherms were obtained at  $-196^\circ\text{C}$  (in liquid N<sub>2</sub>) using a Bellsorp Mini instrument (BEL JAPAN, Inc.). The specific surface areas and the pore volumes of samples were calculated from the adsorption branches of the isotherms

by BET plot and MP method, respectively. The hydrophobicity of each zeolite sample was estimated from the water contact angle of sample powders bedded on XRD glass specimen plate, which were measured by a contact angle meter of EXCIMER Inc., the Model Simage mini, using ATAN1/2θ method. Since smaller volumes of water (less than 10 μL) could not be placed on some hydrophobic powders, an 18 μL of deionized water was dropped onto a zeolite sample to measure the contact angle. In the cases of hydrophilic zeolite samples, the contact angle was unmeasurable because the dropped water was absorbed into the powder shortly. The weight ratios of organic component in zeolite samples were analyzed by a thermogravimetric analyzer (Shimadzu TGA-50) for estimating the contents of the disilane compound and other organic components actually grafted on zeolite samples. All samples were held in a platinum sample holder and were heated from room temperature to 800 °C under air at the rate of temperature increase 3 °C/min. The weight decreases were mainly observed at from 200 to 500 °C, and completed at 600 °C. After deducting the weight loss below 150 °C, the weight decrease from 150 to 600 °C was compared with non-modified HB zeolite (zeolite **1**). For example, while the weight decrease of zeolite **1** from 150 to 600 °C was 0.972%, the decrease of zeolite **5** (10% grafting) was 2.889%. In this case, the weight ratio of the organic component in zeolite **5** was determined to be 1.917%.

## 3. Results and discussion

### 3.1. Modification of HB zeolite with 1,4-bis(hydroxydimethylsilyl) benzene

Fig. 4 shows the nitrogen adsorption isotherms of non-modified (zeolite **1**) and modified HB zeolites with a disilane compound, 1,4-bis(hydroxydimethylsilyl) benzene (zeolites **2–5**). Table 1 summarizes the effect of the disilane modification on the properties of these HB zeolites. In the grafting of the disilane compound onto mordenite and ZSM-5, the specific surface areas and the pore volumes are reduced to less than 10 m<sup>2</sup>/g and 0.001 mL/g, respectively, by complete covering of the exterior surfaces [28–31]. On the other hand, even a zeolite with 10% grafting of the disilane compound had still 436 m<sup>2</sup>/g of surface area and 0.190 mL/g of pore volume

**Table 1**  
Properties of HB zeolite with the modification of 1,4-bis(hydroxydimethylsilyl) benzene.

Zeolite	Ratio of disilane (%) <sup>a</sup>	Specific surface area (m <sup>2</sup> /g) <sup>b</sup>	Pore volume (mL/g) <sup>c</sup>	Weight ratio of organic component (%) <sup>d</sup>	Contact angle (°) <sup>e</sup>
<b>1</b>	–	670.6	0.293	–	Unmeasurable <sup>f</sup>
<b>2</b>	1	580.1	0.259	0.999	Unmeasurable <sup>f</sup>
<b>3</b>	3	554.3	0.245	1.473	127
<b>4</b>	5	514.8	0.225	1.819	139
<b>5</b>	10	436.5	0.190	1.917	136
<b>6<sup>g</sup></b>	0	579.9	0.258	1.428	Unmeasurable <sup>f</sup>

<sup>a</sup> Weight ratio of the disilane compound mixed to HB zeolite in starting composition.

<sup>b</sup> BET surface area.

<sup>c</sup> MP pore volume.

<sup>d</sup> Calculated from the difference from zeolite **1** using results by TGA.

<sup>e</sup> Measured by ATAN1/2θ method using an 18 μL deionized water.

<sup>f</sup> Unmeasurable due to absorption into the powder.

<sup>g</sup> The modification treatment was performed in the absence of 1,4-bis(hydroxydimethylsilyl) benzene.

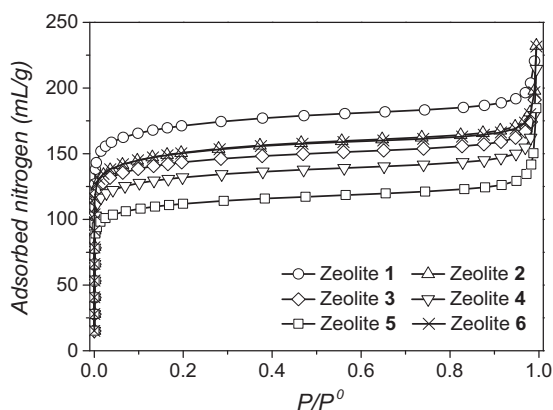


Fig. 4. Nitrogen adsorption isotherms of various HB zeolites (zeolites 1–6)

(zeolite 5). As the pore size of HB zeolite ( $7.6 \times 6.4 \text{ \AA}$ ) is larger than those of mordenite ( $7.0 \times 6.5 \text{ \AA}$ ) and ZSM-5 ( $5.3 \times 5.6 \text{ \AA}$ ), the perfect sealing of the pore outlet was not achieved. However, the good accessibility to the inside of the micropore even after the modification was advantageous to the composite catalyst, because the methanol conversion into  $C_{2+}$  hydrocarbons takes place inside the micropore.

The amounts of grafted organic components on HB zeolite were estimated by thermogravimetric analysis as summarized in Table 1. While the amount of the organic component increased from zeolite 1 to zeolites 2 and 3, no obvious difference was found among zeolites 3–5. The measured weight loss (1.917%) of zeolite 5 was considerably low compared with the estimated weight loss in the case that all disilane compound used is successfully grafted to zeolite 5 (calculated to 4.27%). In these zeolites (zeolites 4 and 5), the whole exterior surface of HB zeolite was still covered with the disilane compound and the excess disilane compound not grafted to zeolite was removed by following methanol washing. The wettability of zeolite samples estimated by water contact angle was significantly changed by the surface modification. An 18  $\mu\text{L}$  water droplet of deionized water was easily absorbed to the powders of zeolite 1 (non-modified) and zeolite 2 (1% grafting), where the contact angles of the droplet were not measurable. On the other hand, the samples with more than 3% grafting (zeolites 3–5) became water repellent to show high contact angles more than  $120^\circ$  as listed in Table 1. Images of these water droplets are illustrated in supplementary data (Fig. S2). Thus, the disilane modification converted the HB zeolite from hydrophilic to hydrophobic. These surface modification had no effect on the crystalline structure and the particle morphology of the zeolite. From the XRD patterns in supplementary data (Fig. S3), no differences of the crystalline structure were found among zeolites 1–5. From scanning electron microscope images illustrated in supplementary data (Fig. S4), the modification process did not change the shape and particle size of HB zeolite. Cubic crystals of HB zeolite ranging from approximately 200 to 800 nm in size were observed in the images before and after the grafting.

### 3.2. Catalytic performance of composite catalysts obtained from disilane modified HB zeolites

Composite catalysts were prepared by physical mixing of a Cu–Zn base oxide as methanol synthesis catalyst with a HB zeolite in a weight ratio of 1:9, which was considered as the most suitable [22]. Table 2 summarizes the results of  $\text{CO}_2$  hydrogenation over these composite catalysts. When a non-modified HB zeolite (zeolite 1) was used in the composite catalyst with Cu–Zn–Al (6:3:1) oxide (run 1), the yield of  $C_{2+}$  hydrocarbons was only 0.48C-mol%

at 2 h of time-on-stream, which was lower than that of oxygenated compounds (methanol and dimethyl ether). This indicated that the transformation of the oxygenated compounds over HB zeolite was considerably restricted. Especially, the formation of a significant amount of dimethyl ether demonstrated that strong acid sites for the transformation of dimethyl ether to  $C_{2+}$  hydrocarbons were seriously damaged, while weak acid sites for the conversion of methanol into dimethyl ether were still active. The negligible yield of methane obtained by the scission of carbon–carbon bond of hydrocarbons was due to the poor formation of  $C_{2+}$  hydrocarbons. When only 0.1 g of Cu–Zn–Al oxide was employed for the reaction (run 2), the yield of the oxygenated compounds (0.75C-mol%; only methanol) was lower than that in run 1. The mixing of zeolite 1 with Cu–Zn–Al oxide modestly promoted the methanol formation from  $\text{CO}_2$  probably because of the equilibrium shift mentioned in the introduction.

When zeolite 2 with 1% grafting of the disilane compound was used in the composite catalyst, the yield of  $C_{2+}$  hydrocarbons was increased to about 5.5C-mol% (run 3). The further grafting (3, 5 and 10%) of the disilane compound enhanced the yield to more than 7C-mol% as listed in runs 4, 6 and 7 (zeolites 3–5). The methane yields over these composite catalysts were low and comparable with the results reported by Fujimoto et al. [6], and the formation of olefins such as ethylene and propylene was very little. The oxygenated compounds were scarcely formed over these composite catalysts. No clear differences in the catalytic activity of these composite catalysts probably resulted from the comparable amount of the grafted disilane compound in zeolites 3–5. These yields of  $C_{2+}$  hydrocarbons were approximately 15 times of that over the composite catalyst using zeolite 1 (non-modified) (run 1) and 20 times higher than the equilibrium conversion of methanol (0.36C-mol%) under the conditions [20]. The production of propane and butane as main LPG components reached about 6C-mol%, and their selectivity was more than 80C-mol% in all  $C_{2+}$  hydrocarbons. Thus, these composite catalysts had a very high catalytic activity for the synthesis of LPG hydrocarbons by  $\text{CO}_2$  hydrogenation. When another modified zeolite prepared by the same procedure as zeolite 4 was used for the reaction, the analogous catalytic activity was found ( $\text{CO}_2$  conversion: 24.43 %,  $C_{2+}$  hydrocarbon yield: 7.55C-mol%). The reproducibility of the grafting process was also ascertained. Although the yield of  $C_{2+}$  hydrocarbons was improved from 0.28 to 2.20C-mol% over the composite catalyst composed of Cu–Zn (3:7) oxide and zeolite 4 (runs 9 and 10), the yield was lower than that over the composite catalyst with Cu–Zn–Al (6:3:1) oxide (run 6). The higher Cu content and the addition of Al might improve the methanol synthesis catalyst used for the composite catalyst.

When the flow rate was reduced in the reaction over the composite catalyst with zeolite 3, the yield and the selectivity of  $C_{2+}$  hydrocarbons became about 12.6C-mol% and 45C-mol%, respectively (run 5). While the increase of  $C_{2+}$  hydrocarbons was about 5.3C-mol%, the increment of  $\text{CO}_2$  conversion was only 2.8%. Since the difference of CO yield between runs 4 and 5 was approximately 2.5C-mol%, it is obvious that the increased  $C_{2+}$  hydrocarbons were compensated both by the decrease of CO yield and the increase of  $\text{CO}_2$  conversion. The longer contact time (slow flow rate) with the zeolite catalyst accelerated methanol conversion to promote the formation of  $C_{2+}$  hydrocarbons. This high transformation of methanol suppressed its decomposition into CO shown in Fig. 2, reducing the yield of CO. Although this higher yield of  $C_{2+}$  hydrocarbons definitely increased water content in the catalytic bed, no equilibrium limitation induced by the water might work in these cases. It is likely that the catalytic hydrogenation of  $\text{CO}_2$  over the composite catalysts with modified zeolites is not controlled by the equilibrium conversion to methanol but those to hydrocarbons, which are much higher than those to methanol and dimethyl ether [6,12]. The best yield of  $C_{2+}$  hydrocarbons obtained under a pressure



**Table 2**  
CO<sub>2</sub> hydrogenation over composite catalysts<sup>a</sup>.

Run	Zeolite	CO <sub>2</sub> conv. (%)	Selectivity (C-mol%)							C <sub>2+</sub> hydrocarbon yield (C-mol%)		
			CO	Hydrocarbon					MeOH			
				C <sub>1</sub>	C <sub>2</sub>	C <sub>3</sub>	C <sub>4</sub>	C <sub>5+</sub>				
1	1	22.63	92.6	<0.1	1.8	0.1	0.2	0.0	3.5	1.8	0.48	
2 <sup>b</sup>	–	17.80	95.8	0.0	0.0	0.0	0.0	0.0	4.2	0.0	0.00	
3	2	24.22	75.0	0.6	2.5	7.7	10.9	1.6	1.3	0.4	5.50	
4	3	24.81	69.5	0.7	3.1	10.7	13.9	1.6	0.4	<0.1	7.27	
5 <sup>c</sup>	3	27.64	53.4	0.7	5.3	17.9	20.0	2.3	0.4	<0.1	12.58	
6	4	24.07	69.2	1.2	3.1	10.2	14.1	1.8	0.4	<0.1	7.03	
7	5	24.92	69.0	1.4	3.3	8.7	15.3	1.8	0.4	<0.1	7.25	
8	6	23.36	82.8	0.5	2.0	4.1	6.4	1.0	2.2	1.0	3.15	
9 <sup>d</sup>	1	21.64	94.1	<0.1	1.3	0.0	0.0	0.0	2.7	1.8	0.28	
10 <sup>d</sup>	4	20.97	87.2	1.2	1.2	4.1	5.2	<0.1	0.9	0.2	2.20	

<sup>a</sup> Catalyst: Cu–Zn–Al (6:3:1) oxide + HB zeolite = 0.1/0.9 (g/g), temperature: 300 °C, pressure: 0.98 MPa, flow rate: 50 mL/min, CO<sub>2</sub>/H<sub>2</sub> = 1/3. Results at 2 h of time-on-stream.

<sup>b</sup> Only 0.1 g of Cu–Zn–Al (6:3:1) oxide was used.

<sup>c</sup> Flow rate: 25 mL/min.

<sup>d</sup> Catalyst: Cu–Zn (3:7) oxide + HB zeolite = 0.1/0.9 (g/g).

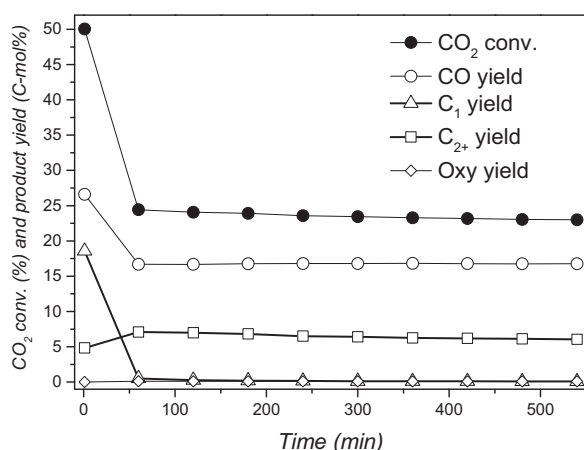


**Fig. 5.** Time courses of CO<sub>2</sub> conversion, the yields of CO, methane (C<sub>1</sub>), C<sub>2+</sub> hydrocarbons and oxygenated compounds (methanol and dimethyl ether) with time-on-stream in the reaction over the composite catalyst using zeolite **4** (run 6 in Table 2).

of 0.98 MPa was approximately equivalent level to the prominent results recently reported by Fujimoto et al. under a pressure of about 2 MPa [6]. Thus, the high yield production of C<sub>2+</sub> hydrocarbons from CO<sub>2</sub> was achieved by using disilane modified zeolite for the composite catalyst with Cu–Zn–Al oxide under a pressure of 0.98 MPa.

### 3.3. Time course of the yields of hydrocarbons

Fig. 5 illustrates the time courses of CO<sub>2</sub> conversion, the yields of CO, methane (C<sub>1</sub>), C<sub>2+</sub> hydrocarbons and oxygenated compounds (methanol and dimethyl ether) over the composite catalyst of Cu–Zn–Al oxide with zeolite **4**. The high production of CO at 1 min of time-on-stream was due to the redox mechanism of reversed-water-gas-shift (RWGS) reaction with freshly formed Cu metal by the pre-reduction [2]. In all the ranges of time-on-stream, the main product was CO. On the other hand, the yield of methane was also prominent at 1 min of time-on-stream (more than 18C-mol%), which decreased rapidly after 1 h to reach below 0.1C-mol% after 9 h. Although the analogous profiles of methane yield were found in other composite catalysts using the disilane modified HB zeolites (zeolites **2**, **3** and **5**), the methane yield at the time was less than 0.1C-mol% over the composite catalyst with zeolite **1** (non-modified). In addition, methane was scarcely detected in the vent gas of the pre-reduction by pure hydrogen flow at 250 °C (less than

0.01C-mol%). The infrared spectra of zeolite **5** and the corresponding composite catalyst used for the catalytic reaction are compared (Fig. S5 in Supplementary data). A clear absorption of zeolite **5** at 1267 cm<sup>−1</sup>, which is assigned to Si–CH<sub>3</sub> bond of the grafted disilane compound [36], disappeared after the use of the reaction. It is thought that the hydrolysis of the Si–CH<sub>3</sub> bond with water formed by CO<sub>2</sub> hydrogenation produced methane found at the initial stage of the reaction, and the decomposition was nearly completed after 9 h. It is noteworthy that no benzene was detected in all catalytic reactions even at 1 min of time-on-stream. No hydrolysis of phenylene group in the disilane compound to benzene progressed during the reaction, and the aromatic ring of the disilane compound still remained in the composite catalyst. On the other hand, the yield of C<sub>2+</sub> hydrocarbons increased at from 1 min to 1 h of time-on-stream and decreased slowly with time after 1 h. The gradual reductions both of CO<sub>2</sub> conversion and C<sub>2+</sub> hydrocarbon yield are thought to result from coke formation usually observed in zeolite catalysts [37,38]. However, C<sub>2+</sub> hydrocarbons were obtained in more than 6C-mol% yield after 9 h. The high catalytic activity for C<sub>2+</sub> hydrocarbon production was maintained even after the decomposition of the Si–CH<sub>3</sub> bond in the grafted disilane compound.

### 3.4. Effect of methanol on catalytic activity

Since methanol was used as solvent in the modification process of the disilane compound, the effect of methanol on the composite catalyst was examined. We prepared another zeolite sample, zeolite **6**, by the similar grafting procedure in the absence of the disilane compound (only methanol was used). This process also decreased the surface area and pore volume of HB zeolite as listed in Table 1. It seems that some derivatives from methanol formed during the modification process reduced the porosity of the zeolite. No variation of the crystalline structure was ascertained from the XRD pattern shown in supplementary data (Fig. S3), and the zeolite powder was still hydrophilic as evidenced by unmeasurable contact angle (Table 1). Although the composite catalyst using zeolite **6** produced C<sub>2+</sub> hydrocarbons in a higher yield than that using zeolite **1** (3.15C-mol%; run 8 of Table 2), the yield was lower than those over the composite catalysts with disilane modified zeolites. In this catalytic reaction, no remarkable formation of methane at 1 min of time-on-stream was found to indicate that the high methane production over the composite catalysts with disilane modified zeolites resulted from the decomposition of the grafted disilane compound. Thus, it was concluded that the surface modification of the disilane compound to HB zeolite substantially improved the

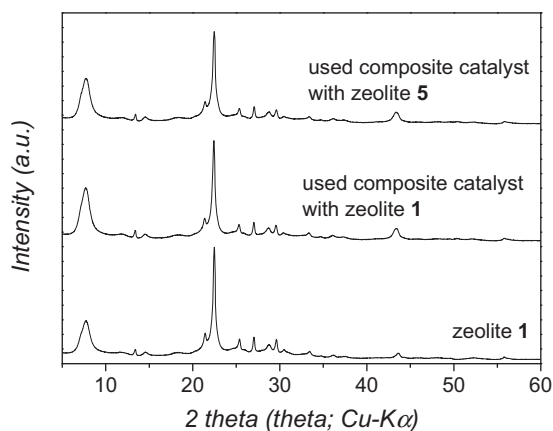


Fig. 6. XRD patterns of zeolite 1, used composite catalysts obtained from zeolites 1 and 5.

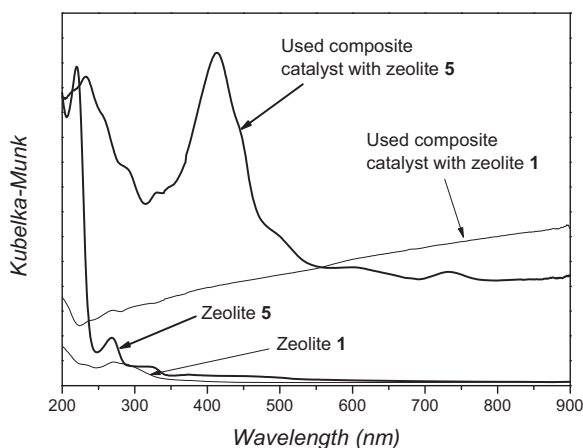


Fig. 7. Diffuse-reflectance UV-vis spectra of zeolite 1, zeolite 5, and used composite catalysts obtained from zeolite 1 and zeolite 5 for the catalytic reaction.

catalytic activity of the corresponding composite catalyst for the synthesis of  $C_{2+}$  hydrocarbons from  $CO_2$ .

### 3.5. Effect of the surface modification on the catalytic activity of composite catalyst

The powder XRD patterns of zeolite 1 and used composite catalysts obtained from zeolites 1 and 5 are illustrated in Fig. 6. The crystalline structure of HB zeolite in the used composite catalysts was nearly the same as that of zeolite 1. It is clear that the poor yield of  $C_{2+}$  hydrocarbons over the composite catalyst using zeolite 1 was not caused from the deterioration of the zeolite structure. The diffraction peaks of Cu–Zn–Al oxide were undetectable in the XRD patterns of these composite catalysts due to its low content (10 wt%). On the other hand, in the XRD pattern of Cu–Zn–Al oxide catalyst used in run 2 of Table 2 (Fig. S6 in Supplementary data), sharp peaks of Cu metal are observed. The crystallization of Cu metal must occur in Cu–Zn–Al oxide of the used composite catalysts as well. Fig. 7 shows diffuse-reflectance (DR) UV-vis spectra of zeolite 1 (non-modified) and zeolite 5 (10% grafting). UV absorption of 1,4-bis(hydroxydimethylsilyl) benzene at 270 nm [28] and an additional absorption around 320 nm in wavelength was observed in zeolite 5. While this additional absorption at 320 nm was also found in the spectra of other modified zeolites 2–4, it was absent in the spectrum of zeolite 1. Fig. 8 illustrates the change of UV absorption of the disilane compound in a diluted methanol solution by the addition of HCl. The original solution of the disilane compound

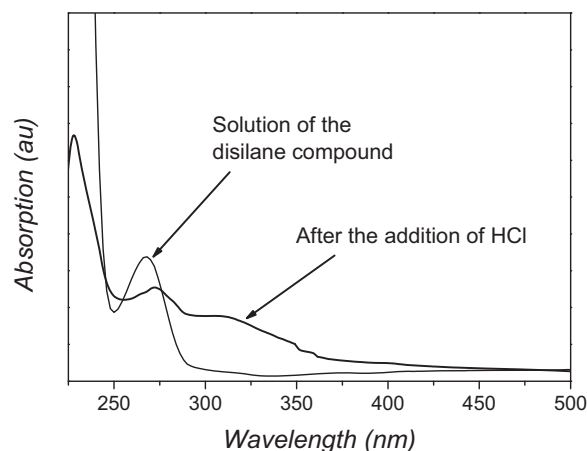
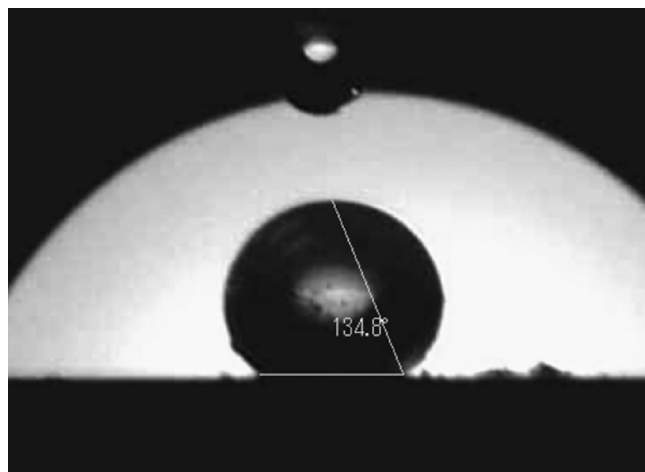


Fig. 8. UV-vis spectra of the disilane compound in methanol before and after addition of HCl.

had an absorption around 270 nm in wavelength that was analogous to the DR UV-vis spectrum depicted in Fig. 7. The addition of a small volume of HCl (a few drops) to the solution decreased the absorption at 270 nm and generated another broad absorption around 320 nm. This variation of UV spectrum seems to result from the protonation of the phenylene group of the disilane compound with HCl. This suggested that the protonation of the grafted disilane compound with acidic zeolite proton produced the absorption around 320 nm in the spectrum of zeolite 5. Fig. 7 also illustrated DR UV-vis spectra of two used composite catalysts with zeolites 1 and 5. These used catalysts became darker in color by the coke formation during the reaction, and their spectra were considerably higher than baseline due to the strong and broad absorption in the UV and visible light range. In the used composite catalyst with zeolite 5, a strong absorption around 420 nm in wavelength was clearly found, which was absent in the used catalyst obtained from zeolite 1. Although the grafted 1,4-bis(hydroxydimethylsilyl) benzene moiety might partly evaporate at the reaction temperature of 300 °C, the new strong absorption around 420 nm indicated that its decomposition also occurred during the reaction. As mentioned in the Section 3.3, the phenylene group in the disilane compound did not decompose to benzene. It is thought that condensed aromatic hydrocarbons obtained from the disilane compound produced the absorption at 420 nm. For example, pyrene has a broad absorption at from 250 to 450 nm in wavelength in solid state [39].

The water repellency of the composite catalysts used for  $CO_2$  hydrogenation was also estimated by water contact angle. The used composite catalysts obtained from zeolite 1 was still hydrophilic to absorb an 18  $\mu$ L water droplet immediately. In addition, Cu–Zn–Al oxide before and after the use of  $CO_2$  hydrogenation also soaked up the water instantly. In the cases of used composite catalysts with zeolites 2 and 3, although the water droplet had high contact angles more than 90°, these droplets were gradually absorbed into the powders for about 20 sec. On the other hand, the water droplet was stable on the used composite catalysts from zeolites 4 and 5, which showed high contact angles more than 130°. The water droplet on the used composite catalyst with zeolite 5 is illustrated in Fig. 9 (contact angle: 135°). Thus, the disilane modified zeolites were still hydrophobic even after the utilization of the catalytic reaction at 300 °C. It is thought that the condensed aromatic hydrocarbon species covering the exterior surface of HB zeolite, which has the absorption at about 420 nm, created the hydrophobicity of the zeolite. This hydrophobic nature of the modified zeolite prevents the deactivation of the acid sites in zeolite by water formed during  $CO_2$  hydrogenation. Consequently, the composite catalyst consisting of the disilane modified HB zeolite had a high catalytic activity for the



**Fig. 9.** Water droplet (18  $\mu$ L) on the used composite catalyst obtained from zeolite 5.

production of  $C_{2+}$  hydrocarbons by  $CO_2$  hydrogenation. The details of the effects of this hydrophobic modification and the application to other zeolites such as ZSM-5 are under examination in our laboratory.

We reported before that the solid–solid interactions between methanol synthesis catalysts and zeolites change the properties of the methanol synthesis catalysts to control the performances of the corresponding composite catalysts [14,18]. Recently, the significant effects of the solid–solid interactions on the catalytic activity of zeolite in composite catalysts are also claimed by other groups [32–35]. For example, the ion exchange of the acidic proton of ZSM-5 with Cu ion from Cu–Zn based catalyst causes the deactivation of the ZSM-5 in composite catalyst [32]. For preventing the solid–solid interaction, the modifications of the exterior surface of each catalysts are examined using silica-coating [32] and core–shell catalysts [40,41], because the interaction mainly takes place at the exterior surface of the catalyst particles. Even in our composite catalyst, the influences of the solid–solid interaction between Cu–Zn–Al oxide and HB zeolite are assumable. Especially, the poor catalytic activity of the composite catalyst with zeolite 1 is likely to be partly due to the effect of the solid–solid interaction. The hydrophobic surface modification of zeolite with the disilane compound is expected to suppress the solid–solid interaction as well, because the hydrophobic surface might prevent the migration of hydrophilic Cu ion.

#### 4. Conclusions

In conclusion, the composite catalysts obtained by the physical mixing with Cu–Zn–Al oxide and HB zeolite that was modified with 1,4-bis(hydroxydimethylsilyl) benzene were very effective for the production of  $C_{2+}$  hydrocarbons by  $CO_2$  hydrogenation. The yields of  $C_{2+}$  hydrocarbons were approximately 15 times compared with the composite catalysts using a non-modified zeolite. The highest yield of  $C_{2+}$  hydrocarbons reached about 12.6C-mol% at 300 °C under a pressure of 0.98 MPa. The modification of zeolite with the disilane compound altered the surface property from hydrophilic to hydrophobic, which was maintained even after the utilization for  $CO_2$  hydrogenation. The preservation of the strong acid sites of HB zeolite with hydrophobic surface improved the catalytic activity for  $CO_2$  hydrogenation. The composite catalyst reported here is expected to contribute the technologies for the energy network using  $CO_2$  and  $C_{2+}$  hydrocarbons, which realizes the reduction of  $CO_2$  emissions and the production of carbon compounds free from fossil fuels using  $CO_2$  as carbon source.

#### Acknowledgments

Authors thank Prof. Takayo K. Moriuchi at Osaka Institute of Technology and Dr. Yasuo Iizuka, a former professor of Kyoto Institute of Technology, for their helps. Authors also acknowledge Dr. Roger Kieffer, a former professor of Strasbourg University, for his supports when authors started the research on  $CO_2$  hydrogenation.

#### Appendix A. Supplementary data

Supplementary data associated with this article can be found, in the online version, at <http://dx.doi.org/10.1016/j.apcatb.2015.05.004>.

#### References

- [1] X.-M. Liu, G.Q. Lu, Z.-F. Yan, J. Beltramini, *Ind. Eng. Chem. Res.* 42 (2003) 6518–6530.
- [2] W. Wang, S. Wang, X. Ma, J. Gong, *Chem. Soc. Rev.* 40 (2011) 3703–3727.
- [3] E.V. Kondratenko, G. Mul, J. Baltrusaitis, G.O. Larrazábal, J. Pérez-Ramírez, *Energy Environ. Sci.* 6 (2013) 3112–3135.
- [4] Y.-N. Li, R. Ma, L.-N. He, Z.-F. Diao, *Catal. Sci. Technol.* 4 (2014) 1498–1512.
- [5] A. Behr, K. Nowakowski, *Catalytic Hydrogenation of Carbon Dioxide to Formic Acid*, Chapter 7 in *Advances in Inorganic Chemistry CO<sub>2</sub> Chemistry*, vol. 66, Academic Press, Waltham, 2014, pp. 223–258.
- [6] C. Li, X. Yuan, K. Fujimoto, *Appl. Catal. A* 475 (2014) 155–160.
- [7] C. Li, K. Fujimoto, *Energy Fuels* 28 (2014) 1331–1337.
- [8] C. Li, X. Yuan, K. Fujimoto, *Appl. Catal. A* 469 (2014) 306–311.
- [9] X. Ni, Y. Tan, Y. Han, N. Tsubaki, *Catal. Commun.* 8 (2007) 1711–1714.
- [10] R. Bai, Y. Tan, Y. Han, *Fuel Process. Technol.* 86 (2004) 293–301.
- [11] Y.-K. Park, K.-C. Park, S.-K. Ihm, *Catal. Today* 44 (1998) 165–173.
- [12] K. Fujimoto, T. Shikada, *Appl. Catal.* 31 (1987) 13–23.
- [13] Y. Tan, M. Fujiwara, H. Ando, Q. Xu, Y. Souma, *Ind. Eng. Chem. Res.* 38 (1999) 3225–3229.
- [14] M. Fujiwara, R. Kieffer, H. Ando, Q. Xu, Y. Souma, *Appl. Catal. A* 154 (1997) 87–101.
- [15] M. Fujiwara, R. Kieffer, L. Udrón, H. Ando, Y. Souma, *Catal. Today* 29 (1996) 343–348.
- [16] M. Fujiwara, H. Ando, M. Matsumoto, Y. Matsumura, M. Tanaka, Y. Souma, *Chem. Lett.* (1995) 839–840.
- [17] M. Fujiwara, H. Ando, M. Tanaka, Y. Souma, *Appl. Catal. A* 130 (1995) 105–116.
- [18] M. Fujiwara, R. Kieffer, H. Ando, Y. Souma, *Appl. Catal. A* 121 (1995) 113–124.
- [19] M. Fujiwara, Y. Souma, *Chem. Commun.* (1992) 767–768.
- [20] W.-J. Shen, K.-W. Jun, H.-S. Choi, K.-W. Lee, *Korean J. Chem. Eng.* 17 (2000) 210–216.
- [21] P.B. Weisz, *Adv. Catal.* 13 (1962) 137–190.
- [22] M. Fujiwara, H. Sakurai, K. Shiokawa, Y. Iizuka, *Catal. Today* 242 (2015) 255–260.
- [23] A.G. Gayubo, A.T. Aguayo, A. Atutxa, R. Prieto, J. Bilbao, *Ind. Eng. Chem. Res.* 43 (2004) 5042–5048.
- [24] K.L. Joshi, G. Psafogiannakis, A.C.T. van Duin, S. Raman, *Phys. Chem. Chem. Phys.* 16 (2014) 18433–18441.
- [25] R. Singh, P.K. Dutta, *Micropor. Mesopor. Mater.* 32 (1999) 29–35.
- [26] P.A. Zapata, J. Faria, M.P. Ruiz, R.E. Jentoft, D.E. Resasco, *J. Am. Chem. Soc.* 134 (2012) 8570–8578.
- [27] P.A. Zapata, Y. Huang, M.A. Gonzalez-Borja, D.E. Resasco, *J. Catal.* 308 (2013) 82–97.
- [28] M. Fujiwara, T. Kitabayashi, K. Shiokawa, T.K. Moriuchi, *Micropor. Mesopor. Mater.* 115 (2008) 556–561.
- [29] M. Fujiwara, T. Kitabayashi, K. Shiokawa, T.K. Moriuchi, *Chem. Eng. J.* 146 (2009) 520–526.
- [30] M. Fujiwara, Y. Fujio, Y. Sato, H. Sakurai, I. Kumakiri, *Micropor. Mesopor. Mater.* 155 (2012) 34–39.
- [31] M. Fujiwara, Y. Fujio, H. Sakurai, H. Senoh, T. Kiyobayashi, *Chem. Eng. Process. Process Intensif.* 79 (2014) 1–6.
- [32] V.V. Ordonsky, M. Cai, V. Sushkevich, S. Moldovác, O. Ersen, C. Lancelot, V. Valtchev, A.Y. Khodakov, *Appl. Catal. A* 486 (2014) 266–275.
- [33] A. García-Trenco, A. Vidal-Moya, A. Martínez, *Catal. Today* 179 (2012) 43–51.
- [34] A. García-Trenco, A. Martínez, *Catal. Today* 227 (2014) 144–153.
- [35] G.R. Moradi, M. Nazari, F. Yaripour, *Fuel Process. Technol.* 89 (2008) 1287–1296.
- [36] Q. Deng, R.B. Moore, K.A. Mauritz, *Chem. Mater.* 7 (1995) 2259–2268.
- [37] M. Stöcker, *Micropor. Mesopor. Mater.* 29 (1999) 3–48.
- [38] U. Olsbye, S. Svelle, M. Bjørgen, P. Beato, T.V.W. Janssens, F. Joensen, S. Bordiga, K.P. Lillerud, *Angew. Chem. Int. Ed.* 51 (2012) 5810–5831.
- [39] M. Fujiwara, K. Shiokawa, T. Kubota, K. Morigaki, *Adv. Powder Technol.* 25 (2014) 1147–1154.
- [40] K. Pinkaew, G. Yang, T. Vitidsant, Y. Jin, C. Zeng, Y. Yoneyama, N. Tsubaki, *Fuel* 111 (2013) 727–732.
- [41] G. Yang, M. Thongkam, T. Vitidsant, Y. Yoneyama, Y. Tan, N. Tsubaki, *Catal. Today* 171 (2011) 229–235.